A study exploring the effects of exercise on cuproptosis targets in Alzheimer's disease brains based on large-scale data

Guang Yang[1,2], Qi Li[1]*

[1]Department of Neurology, The Second Affiliated Hospital of Anhui Medical University, China
[2]Department of Neurology, Kunshan Traditional Chinese Medicine Hospital, China

Submitted: 7 November 2025; **Accepted:** 9 January 2026
Online publication: 16 April 2026

Arch Med Sci
DOI: https://doi.org/10.5114/aoms/216654

***Corresponding author:**
Qi Li
Department of Neurology
The Second Affiliated Hospital of Anhui Medical University
China
E-mail: qili_md@126.com

Abstract

Introduction: Alzheimer's disease (AD) is a progressive neurodegenerative disorder marked by memory loss and cognitive decline. Epidemiological studies have linked sedentary behaviour to increased risk of chronic diseases, but the molecular mechanisms connecting prolonged inactivity to AD remain unclear. Copper dyshomeostasis and a newly defined form of copper-induced cell death – cuproptosis – have been implicated in neurodegeneration. This study investigates the role of cuproptosis-related genes in sedentary elderly individuals and AD patients to identify potential biomarkers and therapeutic targets.

Material and methods: Gene expression profiles from GEO datasets GSE110298 (hippocampus, sedentary AD vs. control) and GSE9103 (skeletal muscle, sedentary vs. active aging) were processed with the limma package ($|\log_2 FC| \geq 1$, adj. $p < 0.05$). Differentially expressed genes (DEGs) were intersected with a curated cuproptosis gene list. KEGG and GO analyses identified enriched pathways. Protein–protein interaction (PPI) networks in Cytoscape highlighted hub genes. Key candidates were validated by quantitative PCR (qPCR) and Western blot in hippocampal and quadriceps tissues of exercise and sedentary mouse models.

Results: In GSE110298 and GSE9103, 2480 and 890 DEGs were identified, respectively, with 90 overlapping genes enriched in mitochondrial metabolism and neurodegeneration pathways. PPI analysis ranked DLD and DLAT as top hubs; these two remained after intersecting with the cuproptosis gene set. Both DLD and DLAT were significantly upregulated in hippocampi of sedentary AD subjects and in skeletal muscle of sedentary aging individuals. qPCR confirmed 1.6- to 2.8-fold mRNA increases for DLD and DLAT ($p < 0.001$), and Western blot showed 1.5- to 2.0-fold protein elevation ($p < 0.05$). Additional modulation of TXN and FDX1 was observed.

Conclusions: Our integrative analysis identifies DLD and DLAT as key cuproptosis markers dysregulated by sedentary behaviour in AD-relevant tissues. These findings implicate copper-driven cell death in linking prolonged inactivity to neurodegeneration, and highlight DLD/DLAT as promising biomarkers and therapeutic targets. Future work should expand cohort validation and dissect mechanistic roles via multi-omics and functional assays.

Key words: exercise, Alzheimer's disease, cuproptosis.

Introduction

Alzheimer's disease (AD) is a complex neurodegenerative disorder characterised by progressive memory loss and cognitive impairment [1, 2]. As the global population ages, the incidence of AD is rising sharply, placing an ever-increasing burden on patients, families, and healthcare systems [3]. A growing body of evidence links a sedentary lifestyle with the development of multiple chronic conditions – such as cardiovascular disease, type 2 diabetes, and various neurodegenerative diseases – but the molecular pathways by which prolonged sitting contributes to AD pathogenesis remain poorly understood [4].

Copper is an indispensable trace element with critical roles in neuronal physiology, including neurotransmitter synthesis, antioxidant defence, and intracellular signalling [5]. However, perturbations in copper homeostasis can become neurotoxic [6]. In AD, aberrant accumulation of copper ions has been observed in affected brain regions; excessive copper may exacerbate neuronal injury by triggering oxidative stress, accelerating amyloid-β (Aβ) aggregation, and activating apoptotic cascades [7]. Moreover, the cellular handling of copper is governed by a network of genes – mutations or dysregulation in these genes may heighten neuronal vulnerability to copper overload, thereby modulating both the risk and the progression of AD [8].

Recently, "cuproptosis" has emerged as a novel form of cell death driven by intracellular copper excess. Cuproptosis entails disruption of mitochondrial metabolism and induction of reactive oxygen species upon copper accumulation, culminating in cell demise [9, 10]. Although cuproptosis has been implicated in cancer, metabolic disorders, and other neurodegenerative conditions, its role at the intersection of sedentary behaviour and AD has not yet been elucidated.

In this study, we aim to identify genes associated with cuproptosis risk in sedentary elderly individuals and in AD patients. By integrating gene-expression profiles from sedentary older adults and from AD cohorts with curated lists of copper-metabolism genes, we seek to uncover the molecular links between copper dysregulation and AD in the context of prolonged sedentary behaviour, thereby revealing novel biomarkers for early diagnosis and potential targets for intervention.

Table I. Information regarding the primers employed in the study

DLAT	5'-GCTGGAGGTGGAAGACTACG-3'
	5'-TCCAGGTAGGCACAGACAAA-3'
DLD	5'-CAGCAGGAGTGCTACAAGGA-3'
	5'-GGCTTCTTGGTCTTGTTGCAT-3'
TXN	5'-AGATCGAGAGCAAGGAAGCG-3'
	5'-TCCAGCTCCACATACGTCATA-3'
FDX1	5'-GGATG GCTGGAAAGGACAG-3'
	5'-CAGGCTGGATGAAAGTGCTT-3'

Methods

GEO Dataset Processing

Data acquisition and DEG identification [11]: We downloaded the GSE110298 and GSE9103 expression datasets from the GEO database. From the published literature, we compiled a gene set closely associated with cuproptosis. Using the limma package in R, we identified differentially expressed genes (DEGs) in each dataset, applying a threshold of $|\log_2 \text{fold change}| \geq 1$ and an adjusted p-value < 0.05.

Pathway enrichment analysis: DEGs were subjected to Gene Ontology (GO) and Kyoto Encyclopaedia of Genes and Genomes (KEGG) pathway enrichment analyses to determine overrepresented biological processes, cellular components, molecular functions, and signalling pathways [12].

PPI network construction: We imported DEGs from GSE110298 and GSE9103 into the Cytoscape database to construct protein–protein interaction (PPI) networks. Hub genes were identified based on network topology metrics (e.g. degree centrality, betweenness).

Intersection of DEGs: To pinpoint robust cuproptosis-related DEGs ("Cu-DEGs"), we took the intersection of DEGs from both GSE110298 and GSE9103.

Expression profiling: Finally, we performed nonparametric analyses on the original expression values to compare the relative abundance of Cu-DEGs across experimental groups within each dataset.

Quantitative PCR (qPCR)

Total RNA was extracted from mouse hippocampus and quadriceps femoris using TRIzol reagent (Beyotime, Shanghai), and residual genomic DNA was removed with DNase I (Thermo Fisher Scientific). RNA concentration and purity were assessed on a NanoDrop ND-1000 spectrophotometer (Thermo Fisher Scientific), with $A_{260}/A_{280} > 1.8$ and $A_{260}/A_{230} > 2.0$ indicating satisfactory purity. One microgram of total RNA was reverse-transcribed into cDNA using the PrimeScript RT Kit (Takara Bio) with a mixture of oligo(dT) and random hexamer primers, following the manufacturer's protocol [13].

Primers for TXN, DLAT, FDX1, DLD, and the reference gene were designed via Primer-BLAST (NCBI) to span exon–exon junctions, thereby minimising the risk of genomic DNA amplification. Primer sequences are presented in Table I.

qPCR reactions were carried out in triplicate using SYBR Green PCR Master Mix (Applied Biosystems) on a QuantStudio 5 real-time PCR system (Thermo Fisher Scientific). Each 20 µl reaction contained 10 µl of SYBR Green Master Mix, 0.5 µM of each forward and reverse primer, and 2 µl of diluted cDNA template. Thermal cycling parameters were as follows: 95°C for 10 min (initial denaturation); 40 cycles of 95°C for 15 s, [annealing temperature]°C for 30 s, and 72°C for 30 s; followed by a melt-curve analysis from 60–95°C at 0.5°C increments to confirm primer specificity. Relative expression levels of target genes were calculated using the $2^{-\Delta\Delta Ct}$ method, with [reference gene name] serving as the internal control. Data from three independent experiments are expressed as mean ± standard deviation.

Western Blot

Tissue samples were lysed in RIPA buffer containing 1% protease inhibitor cocktail (Beyotime) and centrifuged at 12,000 × g for 15 min at 4°C to collect the supernatant. Protein concentrations were determined by BCA assay (Pierce™ BCA Protein Assay Kit) [14]. Equal amounts of protein (20 µg per lane) were separated on 10% SDS–PAGE and transferred to PVDF membranes (Millipore). Membranes were blocked in 5% non-fat milk for 1 h at room temperature, then incubated overnight at 4°C with the following primary antibodies (all from Wuhan Sanying Biotech; dilution 1 : 2000): DLD (catalogue #16431-1-AP); DLAT (catalogue #13426-1-AP); TXN (catalogue #14999-1-AP); FDX1 (catalogue #12592-1-AP); GAPDH (catalogue #60004-1-Ig; internal loading control)

After washing, membranes were incubated with HRP-conjugated secondary antibody (1 : 5000) at room temperature for 1 h. Protein bands were visualised using an ECL chemiluminescence kit (Advansta) and imaged on a ChemiDoc MP system (Bio-Rad). Band intensities were quantified with Image Lab v6.1 software, and target protein levels were normalised to GAPDH. All experiments were performed in triplicate.

Results

Differential gene enrichment analysis and Hub Gene identification

First, we detected 2480 differentially expressed genes (DEGs) in the GSE110298 cohort (Figure 1 A) and 890 DEGs in the GSE9103 cohort (Figure 1 B). Subsequent KEGG pathway analysis of the GSE110298 DEGs revealed the top ten en-

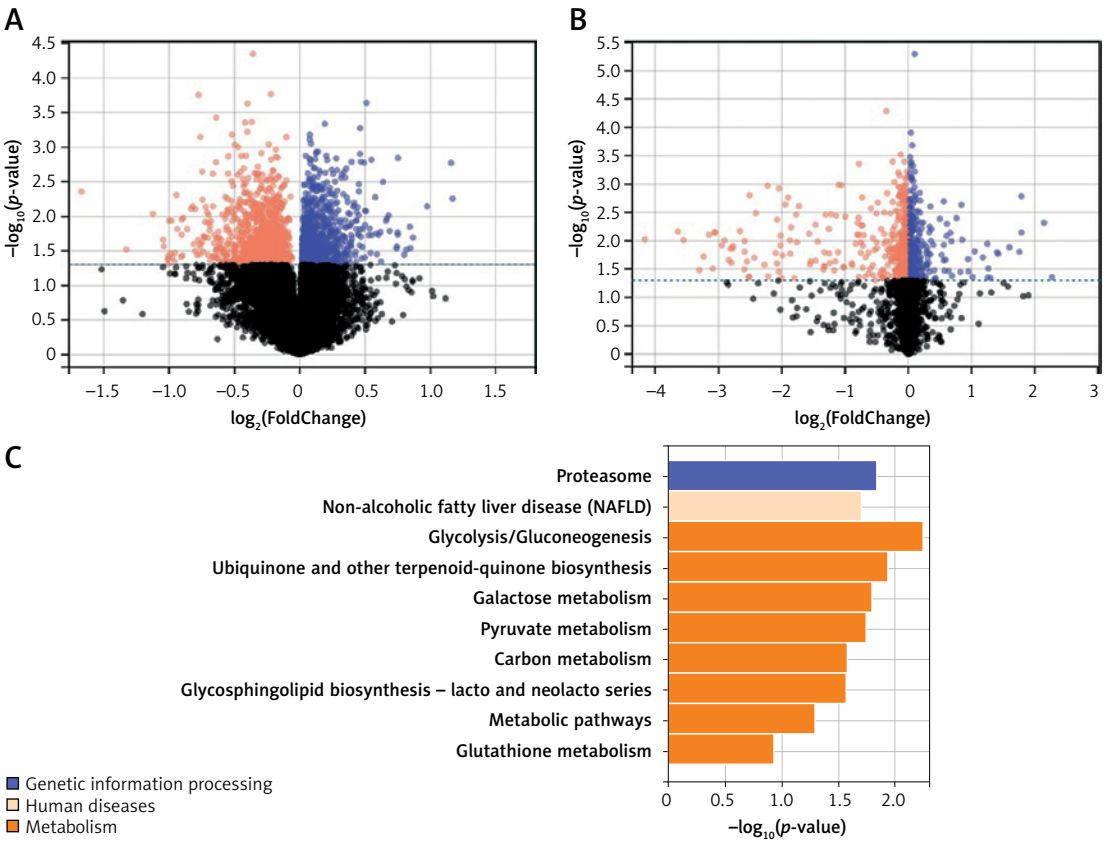

Figure 1. Diagram illustrating the results of the relevant bioinformatics screening process. **A** – Volcano plot of differentially expressed genes in GSE110298. **B** – Volcano plot of differentially expressed genes in GSE9103. **C** – KEGG-associated pathways of differentially expressed genes in GSE110298

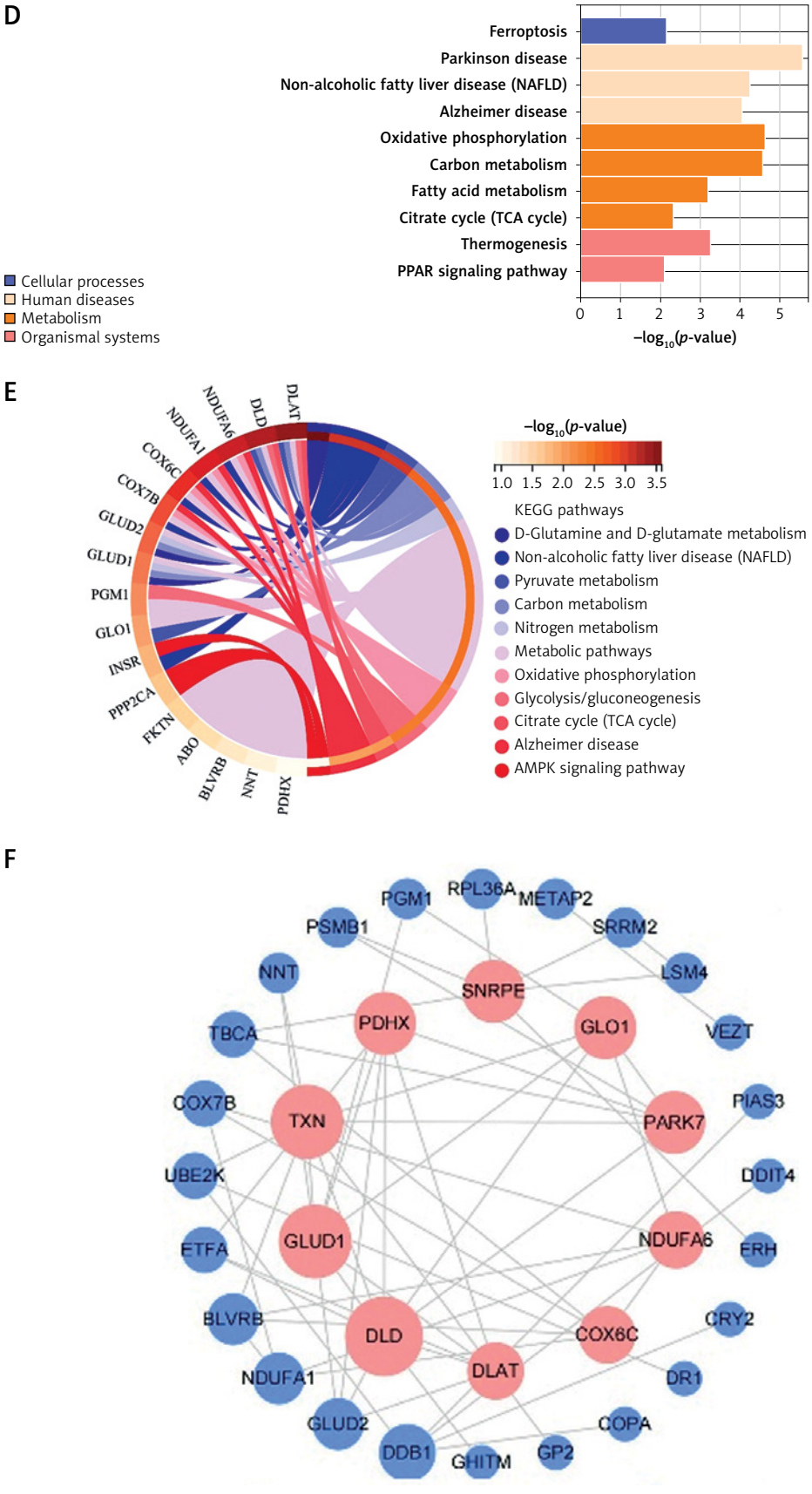

Figure 1. Cont. **D** – KEGG-associated pathways of differentially expressed genes in GSE9103. **E** – KEGG pathways of cuproptosis-associated differentially expressed genes. **F** – Protein-Protein Interaction Network of HUB Gene

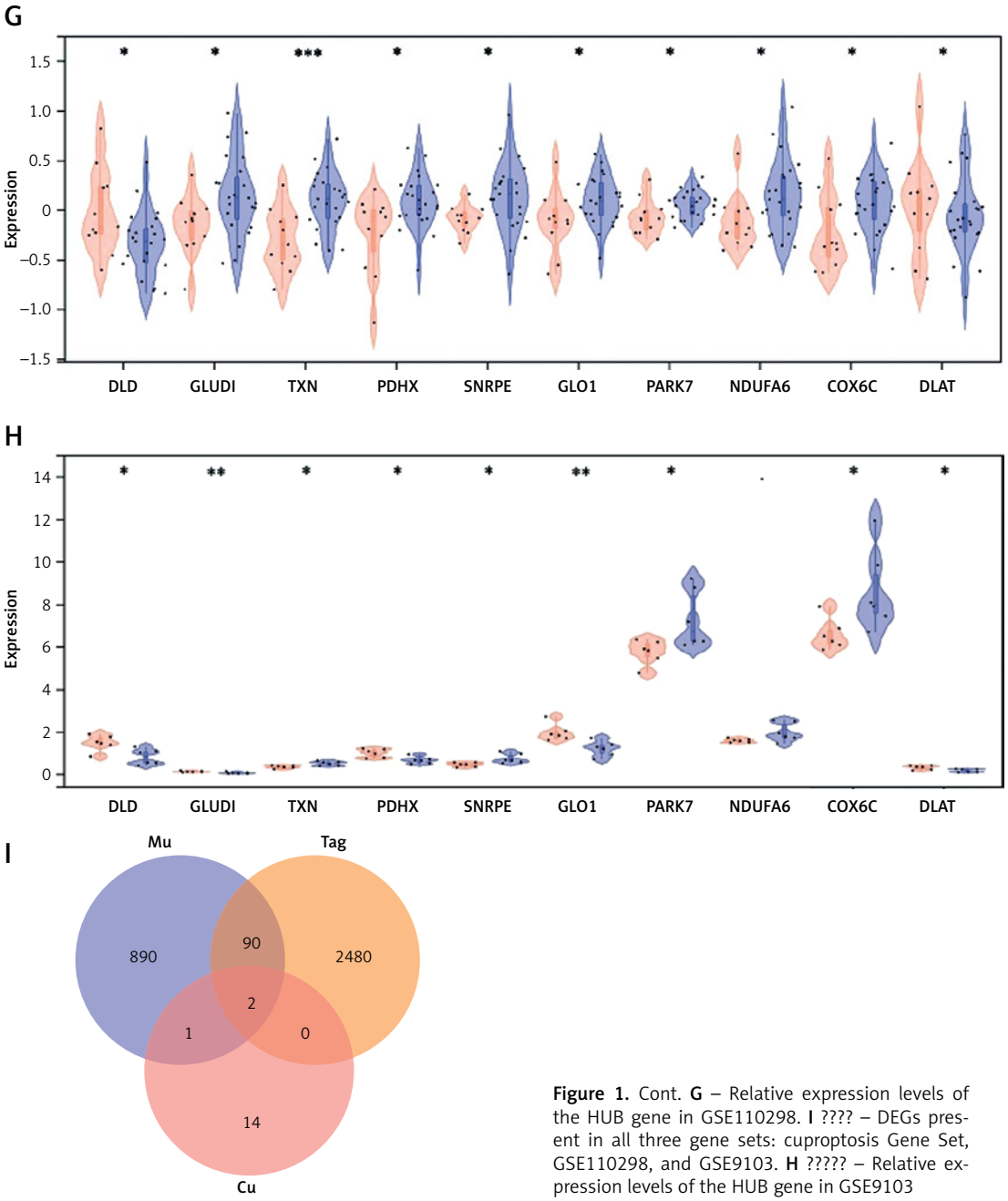

Figure 1. Cont. **G** – Relative expression levels of the HUB gene in GSE110298. **I** ???? – DEGs present in all three gene sets: cuproptosis Gene Set, GSE110298, and GSE9103. **H** ????? – Relative expression levels of the HUB gene in GSE9103

riched pathways to be: proteasome; non-alcoholic fatty liver disease (NAFLD); glycolysis/gluconeogenesis; ubiquinone and other terpenoid-quinone biosynthesis; galactose metabolism; pyruvate metabolism; carbon metabolism; glycosphingolipid biosynthesis – lacto and neolacto series; metabolic pathways; and glutathione metabolism (Figure 1 C). In the GSE9103 dataset, the top ten enriched pathways were ferroptosis; Parkinson's disease; NAFLD; Alzheimer's disease; oxidative phosphorylation; carbon metabolism; fatty acid metabolism; citrate cycle (TCA cycle); thermogenesis; and PPAR signalling pathway. Notably, several pathways – such as NAFLD and carbon metabolism – were shared between the two datasets, suggesting common molecular perturbations.

Next, we took the intersection of the two DEG lists, yielding 90 genes that were differentially expressed in both cohorts. KEGG analysis of these 90 overlapping DEGs highlighted pathways including the TCA cycle, pyruvate metabolism, and Alzheimer's disease (Figure 1 E), strongly implicating dysregulation of mitochondrial metabolism and neurodegenerative processes potentially linked to cuproptosis.

We then constructed a protein–protein interaction (PPI) network from these 90 co-DEGs. The top ten nodes by degree centrality were DLD, GLUD1,

TXN, PDHX, SNRPE, GLO1, PARK7, NDUFA6, COX6C, and DLAT –among which DLD and DLAT have been characterised as key cuproptosis marker genes. Finally, when we intersected our DEG list with the curated cuproptosis-related gene set, only DLD and DLAT remained (Figure 1 I), consistent with their established roles in copper-induced cell death.

Finally, we assessed the expression levels of DLD and DLAT in both datasets. As shown in Figure 1 G, in the GSE110298 cohort, both DLD and DLAT were significantly upregulated in sedentary AD subjects compared with controls. Likewise, in GSE9103 (Figure 1 H), DLD and DLAT were highly expressed in the skeletal muscle of sedentary aging individuals. Taken together, these findings suggest that cuproptosis may be activated in the hippocampus of sedentary AD subjects and in the skeletal muscle of sedentary elderly individuals, potentially exacerbating disease progression.

qPCR Validation

To validate these bioinformatic findings at the mRNA level, we performed quantitative PCR on hippocampal and quadriceps femoris tissues from exercise and sedentary mouse groups (Figure 2).

DLD: Hippocampus: exercise group, 1.35 ±0.07; sedentary group, 2.24 ±0.09 ($p < 0.001$). Quadriceps: exercise group, 1.48 ±0.05; sedentary group, 2.63 ±0.12 ($p < 0.0001$).

DLAT: Hippocampus: exercise group, 1.09 ±0.06; sedentary group, 2.24 ±0.09 ($p < 0.001$). Quadriceps: exercise group, 1.13 ±0.05; sedentary group, 2.31 ±0.11 ($p < 0.0001$).

Additionally, we examined two other genes – TXN and FDX1 – often linked to cuproptosis but not flagged as DEGs in our enrichment analysis, based on previous reports of their importance in copper-induced cell death: TXN: Hippocampus: exercise group, 1.69 ±0.04; sedentary group, 0.91

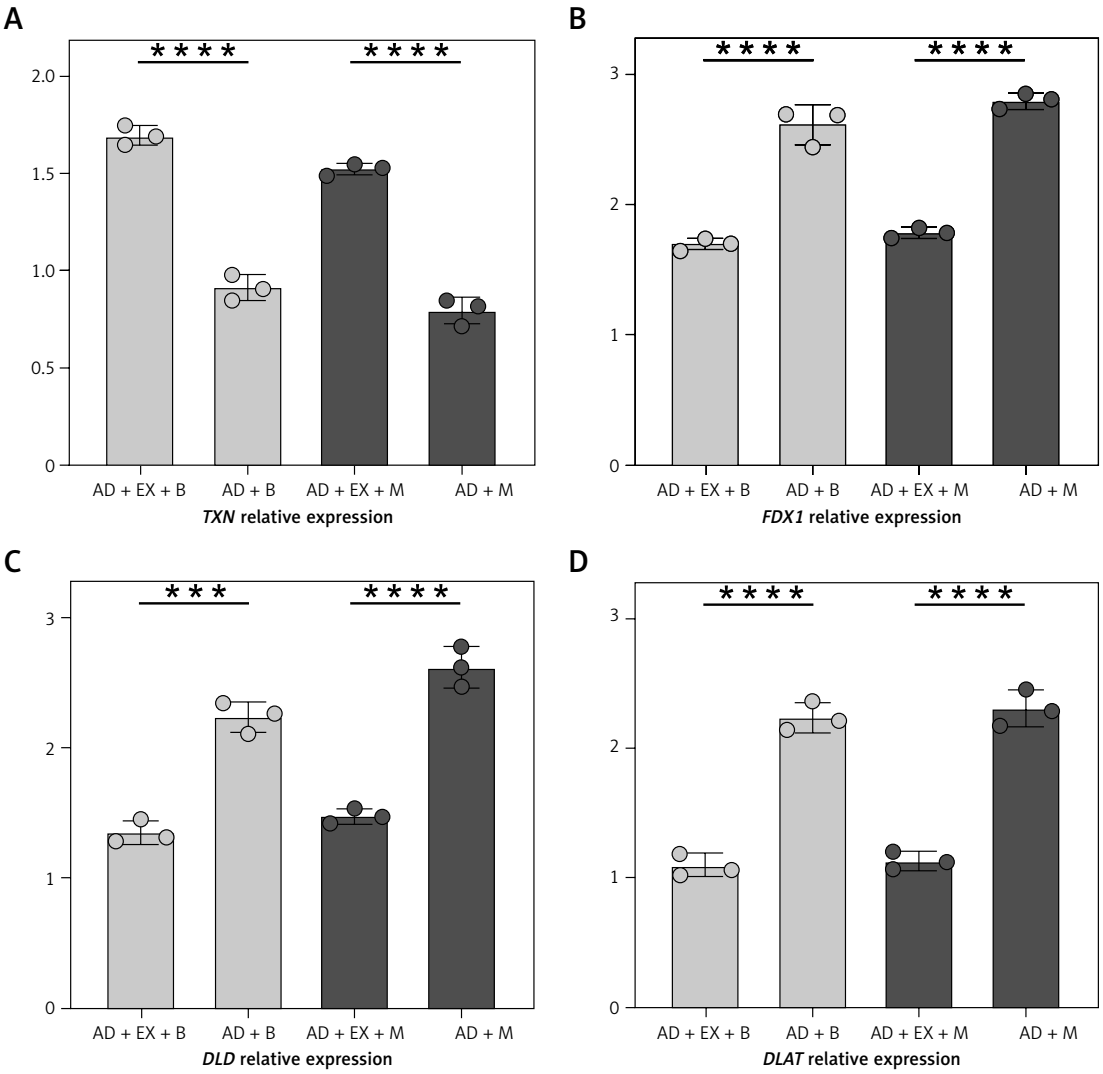

Figure 2. The results of qPCR: **A** – the results of TXN, **B** – the results of FDX1, **C** – the results of DLD. **D** – the results of DLAT

±0.09 ($p < 0.001$). Quadriceps: exercise group, 1.52 ±0.02; sedentary group, 0.79 ±0.06 ($p < 0.0001$).

FDX1: Hippocampus: exercise group, 1.69 ±0.03; sedentary group, 2.61 ±0.12 ($p < 0.001$). Quadriceps: exercise group, 1.78 ±0.03; sedentary group, 2.79 ±0.04 ($p < 0.0001$).

These qPCR results corroborate the upregulation of DLD and DLAT in both hippocampal and skeletal muscle tissues under sedentary conditions and reveal additional modulation of TXN and FDX1, further implicating cuproptosis-related pathways in the detrimental effects of prolonged inactivity.

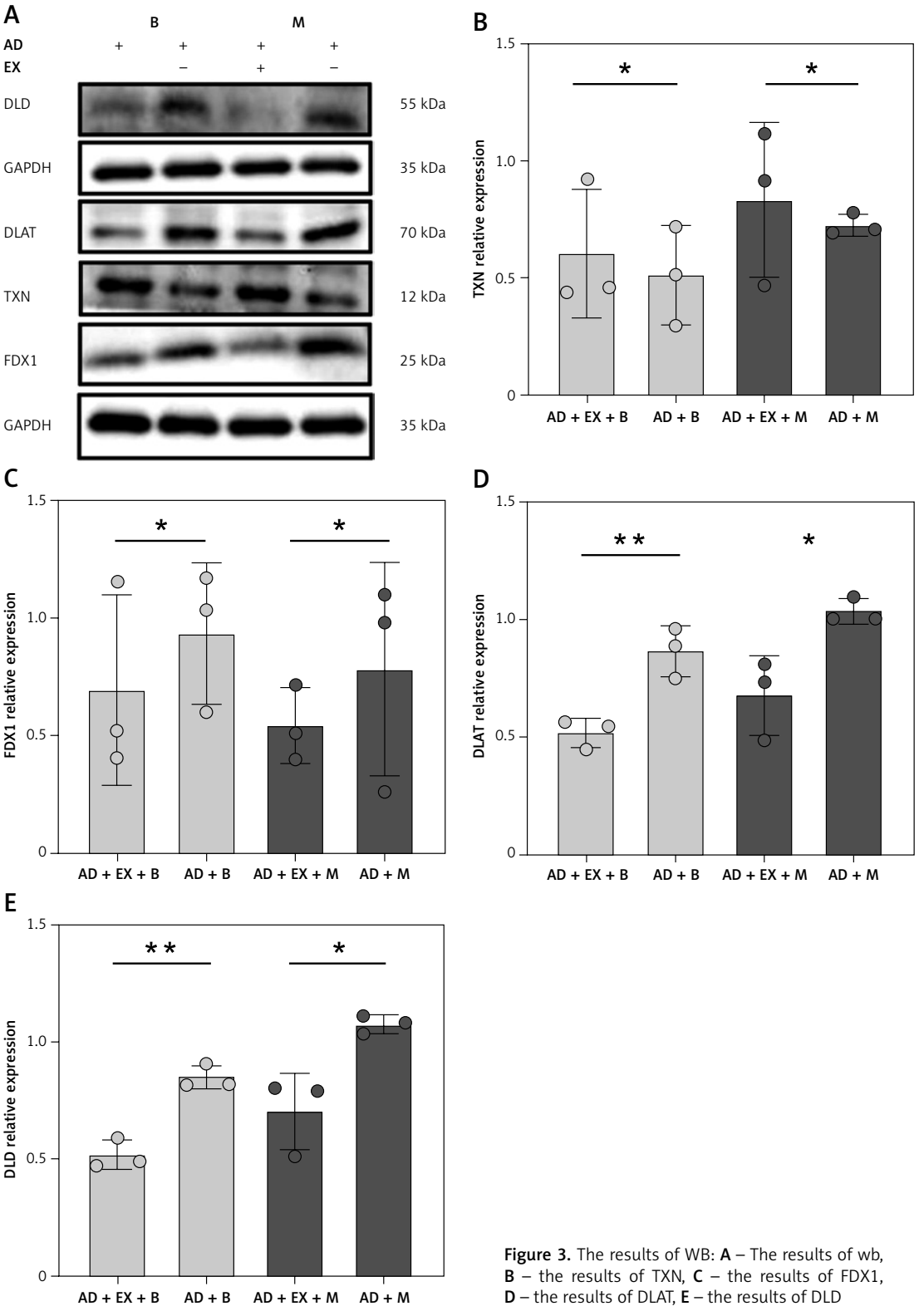

Figure 3. The results of WB: **A** – The results of wb, **B** – the results of TXN, **C** – the results of FDX1, **D** – the results of DLAT, **E** – the results of DLD

Western Blot

Because our qPCR results demonstrated significant transcriptional differences between exercise and sedentary groups, we next examined whether these changes were recapitulated at the protein level. As shown in Figure 3:

DLD: Hippocampus: exercise group, 0.51 ±0.06; sedentary group, 0.85 ±0.05 ($p < 0.05$). Quadriceps femoris: exercise group, 0.70 ±0.16; sedentary group, 1.07 ±0.03 ($p < 0.05$).

DLAT: Hippocampus: exercise group, 0.52 ±0.06; sedentary group, 0.86 ±0.11 ($p < 0.05$). Quadriceps femoris: exercise group, 0.68 ±0.16; sedentary group, 1.03 ±0.05 ($p < 0.05$).

TXN: Hippocampus: exercise group, 0.60 ±0.27; sedentary group, 0.51 ±0.21 ($p < 0.05$). Quadriceps femoris: exercise group, 0.83 ±0.33; sedentary group, 0.72 ±0.04 ($p < 0.05$).

FDX1: Hippocampus: exercise group, 0.69 ±0.40; sedentary group, 0.93 ±0.29 ($p < 0.05$). Quadriceps femoris: exercise group, 0.54 ±0.16; sedentary group, 0.78 ±0.45 ($p < 0.05$).

In all cases, protein expressions of DLD, DLAT, TXN, and FDX1 were significantly higher (or altered) in sedentary mice compared with their exercising counterparts, consistent with the mRNA-level findings and supporting a role for these cuproptosis-related proteins in mediating the molecular effects of prolonged inactivity.

Discussion

In this study, we identified DLD and DLAT as key marker genes of cuproptosis. Their marked upregulation in the hippocampus of sedentary AD patients and in the skeletal muscle of sedentary elderly individuals suggests that copper-induced cell death may be activated in these tissues, potentially accelerating disease progression.

Our findings align with previous reports implicating dysregulated copper homeostasis in AD pathogenesis. Prior work has documented the aberrant accumulation of copper ions in the brains of AD patients and its contribution to oxidative stress and neuronal toxicity [15]. Here, we extend those observations by demonstrating that a sedentary lifestyle can further exacerbate copper toxicity through the altered expression of specific copper-metabolism genes, thereby elevating AD risk. Notably, among the cuproptosis-related genes we uncovered, DLD [16, 17] and DLAT have not been extensively studied in the context of AD [18, 19]; this is, to our knowledge, the first report linking their dysregulation to both cuproptosis and Alzheimer's disease, opening new avenues for mechanistic investigation.

Despite these important insights, our study has several limitations. First, the sample size in both the GEO cohorts and our animal experiments was modest, which may constrain the statistical power and generalizability of our conclusions. Future studies should employ larger, independent cohorts to validate these results [20, 21]. Second, our work focused primarily on transcriptomic analyses, with only preliminary protein-level confirmation. Comprehensive functional validation – through proteomic profiling, cellular assays, and *in vivo* models – will be essential to establish causal roles for these cuproptosis genes in mediating the effects of sedentary behaviour on neurodegeneration [22]. Third, we did not account for other potentially confounding variables such as diet, medication use, or comorbid conditions, all of which can influence copper metabolism and gene expression. Subsequent research should integrate these factors to more fully elucidate the molecular mechanisms linking prolonged inactivity to AD onset and progression. However, in practice, copper chelating agents frequently appear in relevant studies as a validation condition [5]. It is regrettable that this study failed to employ this method to further explore the associated findings, but it is hoped that future research may address this omission.

Looking forward, several lines of inquiry will be particularly fruitful. Gene-editing approaches (e.g. CRISPR-Cas9-mediated knockout or overexpression) could dissect the specific contributions of DLD, DLAT, and other cuproptosis-related genes to copper transport, reactive oxygen species generation, and apoptosis. Integrative multi-omics strategies – combining metabolomics, proteomics, and transcriptomics – will enable reconstruction of the complex molecular networks underpinning copper dysregulation in AD. Finally, given the global prevalence of sedentary behaviour, translational efforts should evaluate interventions aimed at restoring copper homeostasis – such as tailored exercise regimens, dietary modulation of copper intake, or pharmacological chelators – to prevent or delay the onset and progression of Alzheimer's disease.

In conclusion, our integrative analysis identifies DLD and DLAT as key cuproptosis markers dysregulated by sedentary behaviour in AD-relevant tissues. These findings implicate copper-driven cell death in linking prolonged inactivity to neurodegeneration and highlight DLD/DLAT as promising biomarkers and therapeutic targets. Future work should expand cohort validation and dissect mechanistic roles via multi-omics and functional assays.

Funding

This research was supported Suzhou City Applied Basic Research and Science and Technology Innovation Project (SYWD2024196).

Ethical approval

Approval number: 20240827-0055-01.

Conflict of interest

The authors declare no conflict of interest.

References

1. Zhang XX, Tian Y, Wang ZT, Ma YH, Tan L, Yu JT. The epidemiology of Alzheimer's disease modifiable risk factors and prevention. J Prev Alzheimers Dis 2021; 8: 313-21,
2. Lin M, Zhou Y, Liang P, et al. Identification of Alzheimer's disease biomarkers and their immune function characterization. Arch Med Sci 2025; 21: 233-57.
3. Lane CA, Hardy J, Schott JM. Alzheimer's disease. Eur J Neurol 2018; 25: 59-70.
4. Wallace LMK, Theou O, Godin J, Andrew MK, Bennett DA, Rockwood K. Investigation of frailty as a moderator of the relationship between neuropathology and dementia in Alzheimer's disease: a cross-sectional analysis of data from the rush memory and aging project. Lancet Neurol 2019; 18: 177-84.
5. Meng D, Luo G, Liu P. Copper metabolism and cuproptosis in Alzheimer's disease: mechanisms and therapeutic potential. Biomed Pharmacother 2025; 190: 118354.
6. Sensi SL, Granzotto A, Siotto M, Squitti R. Copper and zinc dysregulation in Alzheimer's disease. Trends Pharmacol Sci 2018; 39: 1049-63.
7. Scheiber IF, Mercer JFB, Dringen R. Metabolism and Functions of copper in brain. Prog Neurobiol 2014; 116: 33-57.
8. Roy RG, Mandal PK, Maroon JC. Oxidative stress occurs prior to amyloid Aβ plaque formation and tau phosphorylation in Alzheimer's disease: role of glutathione and metal ions. ACS Chem Neurosci 2023; 14: 2944-54.
9. Chen L, Min J, Wang F. Copper homeostasis and cuproptosis in health and disease. Signal Transduct Target Ther 2022; 7: 378.
10. The Molecular Mechanisms of Cuproptosis and Its Relevance to Cardiovascular Disease-All Databases Available online: https://webofscience.clarivate.cn/wos/alldb/full-record/WOS:001001322300001 (accessed on 28 April 2025).
11. Home - GEO - NCBI Available online: https://www.ncbi.nlm.nih.gov/geo/ (accessed on 28 April 2025).
12. Kanehisa, M, Furumichi, M, Sato, Y, Kawashima, M, Ishiguro-Watanabe, M. KEGG for taxonomy-based analysis of pathways and genomes. Nucleic Acids Res 2023; 51: D587-92.
13. Everaert C, Luypaert M, Maag JLV, et al. Benchmarking of RNA-sequencing analysis workflows using whole transcriptome RT-qPCR expression data. Sci Rep 2017; 7: 1559.
14. Pillai-Kastoori L, Schutz-Geschwender AR, Harford JA. A systematic approach to quantitative western blot analysis. Anal Biochem 2020; 593: 113608.
15. Zhang E, Dai F, Chen T, Liu S, Xiao C, Shen X. Diagnostic models and predictive drugs associated with cuproptosis hub genes in Alzheimer's disease. Front Neurol 2023; 13: 1064639,
16. Ahmad W, Ebert PR. Suppression of a Core metabolic enzyme dihydrolipoamide dehydrogenase (Dld) protects against amyloid beta toxicity in C. elegans model of Alzheimer's disease. Genes Dis 2021; 8: 849-66.
17. Brown AM, Gordon D, Lee H, et al. Testing for linkage and association across the dihydrolipoyl dehydrogenase gene region with Alzheimer's disease in three sample populations. Neurochem Res 2007; 32: 857-69.
18. Chen G, Xi E, Gu X, Wang H, Tang Q. The study on cuproptosis in Alzheimer's disease based on the cuproptosis key gene FDX1. Front Aging Neurosci 2024; 16: 1480332.
19. Copper induces cognitive impairment in mice via modulation of cuproptosis and CREB signaling-All Databases Available online: https://webofscience.clarivate.cn/wos/alldb/full-record/WOS:000940959500001 (accessed on 28 April 2025).
20. Agarwal R, Kushwaha SS, Tripathi CB, Singh N, Chhillar N. Serum copper in Alzheimer's disease and vascular dementia. Indian J Clin Biochem 2008; 23: 369-74.
21. AIBL research group; Rembach A, Doecke JD, Roberts BR, et al. Longitudinal analysis of serum copper and ceruloplasmin in Alzheimer's disease. J Alzheimers Dis 2013; 34: 171-82.
22. Rakhra G, Masih D, Vats A, et al. Effect of physical activity and age on plasma copper, zinc, iron, and magnesium concentration in physically active healthy males. Nutrition 2017; 43-44: 75-82.